Dear Reviewer,

We sincerely thank the reviewer for their time and effort in reviewing our manuscript and for providing valuable comments and constructive suggestions. We appreciate the recognition of our work and the suggestions offered to improve its clarity and scientific rigor. In the responses below, the reviewer's original comments are reproduced in *italic* for clarity. Our point-by-point replies follow each comment and are marked in green. All corresponding changes have been made in the revised manuscript and are marked in blue. Line numbers refer to the revised manuscript unless otherwise noted.

General comments:

PMF analysis is a widely used receptor model for source apportionment. Running bin-PMF for subranges is an interesting combination to extract more detailed information from the CIMS dataset, where both the sources and sinks can vary greatly. However, the interpretation of the solutions requires great efforts and experience. Although the manuscript is well-structured, several parts of the manuscript need improvement and more detailed clarification. Therefore, I recommend a major revision before the manuscript can be considered for acceptance.

Specific/technical comments:

Line 145. The assumption that "OOMs detected have the same ionization efficiency as H_2SO_4" may not be valid. Previous quantum chemical computations (Hyttinen et al., 2015) have shown that in order to be detected effectively by NO_3, the highly oxygenated organic molecules need to contain two H-donor functional groups to reach collision-limited detection (typically, at least 7-8 O atoms). However, you "observed OOMs include 3–6 effective oxygen atoms, accounting for 85% of the total signals" (line 206). Can you estimate, at least, the measurement uncertainty introduced by your assumption?

Response:

We thank the reviewer for this insightful comment. We agree that the assumption of collision-limited detection efficiency comparable to H_2SO_4 only strictly applies to HOMs, typically with at least 7–8 oxygen atoms and multiple hydrogen donor groups (Hyttinen et al., 2015; Riva et al., 2019). Moderate oxygenated compounds (i.e., with fewer oxygen atoms or lacking strong hydrogen donor groups) may indeed experience lower detection efficiency with the NO_3^- ion, leading to potential underestimation of their actual ambient concentrations. Riva et al. (2019) illustrated this point by measuring α-pinene ozonolysis products, showing that Nitrate CI-APi-TOF tends to underestimate species with lower oxygen content compared to other ionization methods (Fig. R1). If these monoterpene products are representative of OOMs, Nitrate CI-APi-TOF may significantly underestimate OOMs with lower oxygen numbers, resulting in differences in magnitude compared to other chemical ionization techniques.

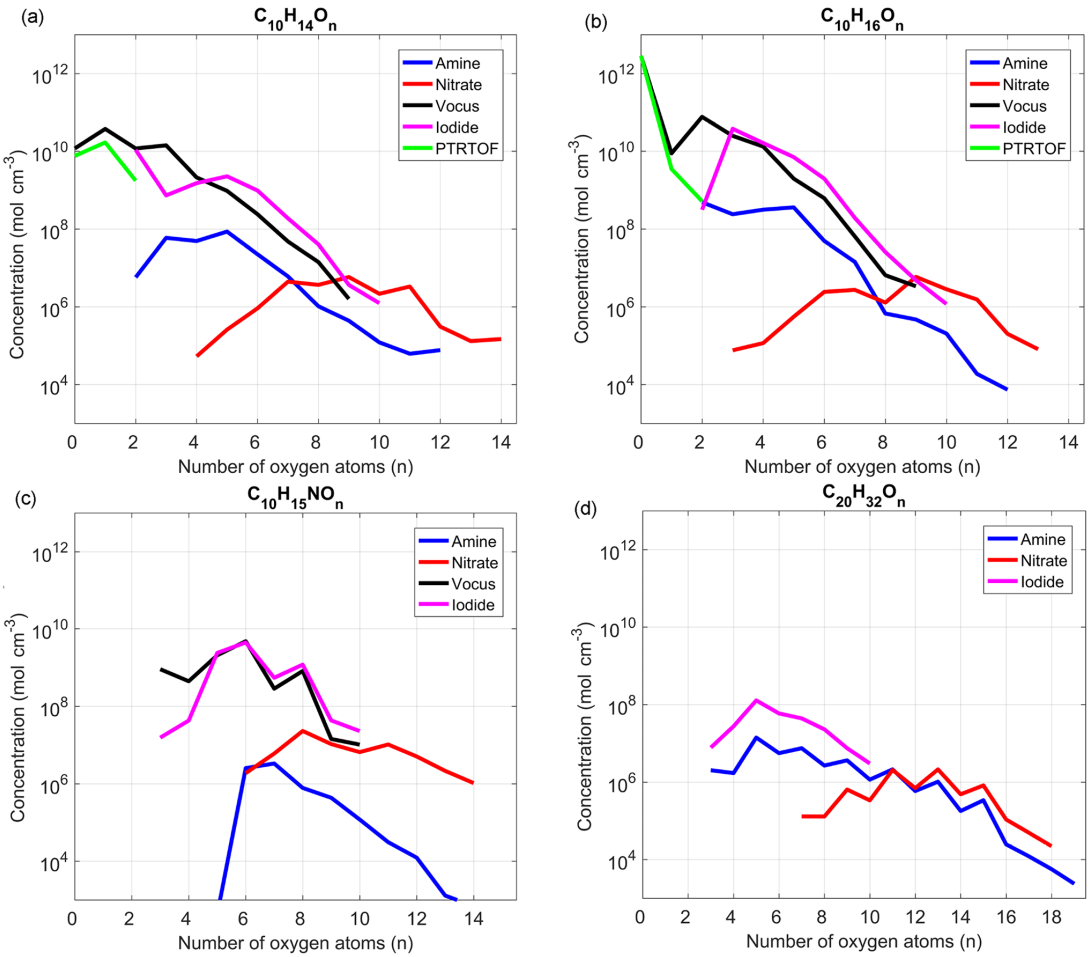

Figure R1. Estimated concentrations of the main α-Pinene C10-monomer oxidation products (a, b), C10-monomer organonitrates (c) and α-Pinene dimers (d) by the different mass spectrometers deployed in Riva et al. (2019).

To clarify this point, our earlier mention that 85% of the detected OOM signals fall in the range of 3-6 effective oxygen atoms was based on the functional-group-adjusted oxygen count used for volatility estimation (which does not include nitrate groups). However, when considering the actual number of oxygen atoms in the molecular formulas, the distribution shifts toward higher oxygenation. As shown in the pie chart below (Fig. R2), over half of the total signals are contributed by OOMs with $n_O \geq 7$, which more reasonably satisfies the criteria for efficient NO_3^- ionization. We acknowledge that the remaining of the detected signals may have a lower ionization efficiency, potentially leading to underestimation of their true concentrations. Given current instrumental limitations, it is difficult to precisely quantify the extent of underestimation across the all OOMs. Still, the assumption of H_2SO_4-like ionization efficiency remains the most practical and widely used approach for semi-quantitative analysis in Nitrate CI-APi-TOF studies. Since our work focuses primarily on source apportionment and chemical evolution trends rather than absolute quantification, we believe this assumption is reasonable and does not compromise the central conclusions. This point has been clarified in the revised manuscript.

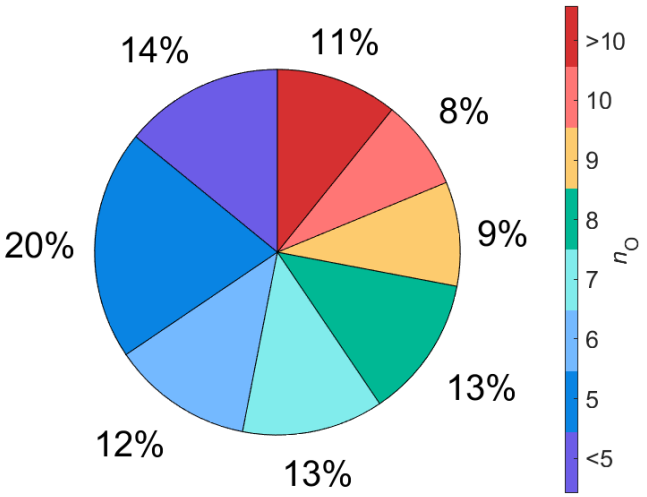

Figure R2. Distribution of the number of oxygen atoms (n_O) for all OOMs identified in this study.

Revised text:

Page 4, Line 145-153: This assumption is generally valid for highly oxygenated molecules (typically with more than 6 oxygen atoms) due to their efficient clustering with NO_3^- (Hyttinen et al., 2015; Riva et al., 2019). However, for less oxygenated compounds—particularly those with fewer than six oxygen atoms—ionization efficiency can be substantially lower, resulting in an underestimation of their true concentrations. Although some uncertainty remains in quantifying moderately oxidized species, the assumption remains the most practical and widely used approach for semi-quantitative analysis in related studies.

Page 4, Section 2.2 instrumentation. Did you use an Eisle NO_3 inlet for NO_3-CIMS? What was the time resolution of the CIMS dataset used for the PMF analysis? And what are the flow settings for the instruments (e.g., NO3-CIMS, PTR, TOF-ACSM…, maybe summarize the details in a table in the supplementary)? It could also be useful if you could include some of the results/figures on your SA calibration and transmission tests in the supplementary. All these experimental details are important for data quality assessment and inter-study comparisons.

Response:

We thank the reviewer for pointing out the importance of providing more detailed instrumental information. In this study, the Nitrate-CIMS utilized the Eisele-type NO_3^- inlet. The raw data were acquired at a frequency of 1 Hz, and averaged to 30-minute intervals for the PMF analysis. The flow settings for CIMS and other supporting instruments have now been summarized in Table S1 in the Supplementary Information.

Although the ACSM was operated during the campaign, its data were not used in the current analysis. Therefore, we have removed related text from the main manuscript to avoid confusion.

In addition, the calibration results for sulfuric acid and the mass-dependent transmission efficiency test of the APi-TOF have also been included in the Supplement (Fig. S1), as suggested.

Revised text:

Page 5, Line 170-172: More details about the instruments can be found in the Supplementary Information, including the flow settings of each instrument and the results of the sulfuric acid calibration and transmission efficiency characterization of the CI-APi-TOF (Fig. S1).

Page 2, Line 30-53 (SI):

S1 Additional details for the instruments

S1.1 Flow settings of the instruments

For the CI-APi-TOF measurements, ambient air was drawn into a laminar flow reactor through a stainless-steel tube (100 cm long, 3/4 in. diameter) at a flow rate of 10 L/min. A sheath flow of 25 L/min of purified airflow was used to maintain laminar flow conditions within the reactor. Nitrate reagent ions were generated in the sheath flow by exposing air-conditioning nitric acid to a photoionizer X-ray (Model L9491, Hamamatsu, Japan). The PTR-TOF-MS sampled air at a flow rate of 200 mL/min and was connected to an external pump operating at 1.5 L/min to assist in flow control. Flow settings and additional details for other instruments used in this study are summarized in Table S1.

Table S1. Settings for instrumentations used in this study

Measurement	Instruments	Manufacturer	Sample flow	Resolustion
OOMs	CI-APi-TOF	Aerodyne Research, USA/ Tofwerk AG, Switzerland	10 L/min	30 min/1s
VOCs	PTR-TOF	Ion-icon Analytik, Austria	0.2 L/min	10 min/1min
$PM_{2.5}$	SHARP-5030	Thermo Fisher Scientific, USA	16.7 L/min	5 min
O_3	TEI-49i	Thermo Fisher Scientific, USA	0.7 L/min	5 min/1 min
NO_x	TEI-42i	Thermo Fisher Scientific, USA	1.285 L/min	5 min/1 min
SO_2	TEI-43C	Thermo Fisher Scientific, USA	0.5 L/min	5 min/1 min
CO	TEI-48C	Thermo Fisher Scientific, USA	1 L/min	5 min/1 min

S1.2 Sulfuric acid calibration and transmission test

The sulfuric acid calibration factor used in this study was obtained following the method described by Kürten et al. (2012), and the results are shown in Fig. S1. The

transmission efficiency of the CI-APi-TOF as a function of mass was evaluated using perfluorinated organic acids, including Propanoic acid, Pentanoic acid, and Heptanoic acid. The outcome of the transmission test is also presented in Fig. S1.

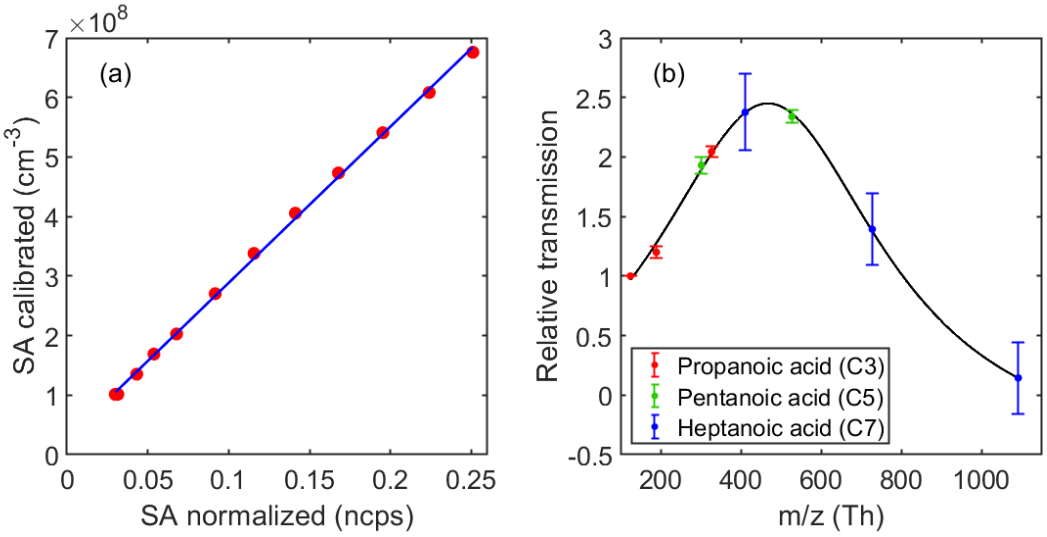

Figure S1. (a) Calibration of sulfuric acid (SA) using the method described by Kürten et al. (2012). (b) Mass-dependent transmission efficiency of the CI-APi-TOF.

Section 3.2.2. For factor D2-AVOC-II, the diurnal variation is bimodal. Why do you think PMF analysis failed to separate this factor into two different factors, one multi-generational oxidation product peaking around 13:00, and one NO_3 oxidation of CHNO compounds peaking around 19:00? Since they have different time variations, PMF should, in principle, be able to distinguish them, right?

Response:

We appreciate the reviewer's thoughtful suggestion. The bimodal diurnal pattern of D2-AVOC-II indeed suggests potential influences from both daytime OH-driven oxidation and nighttime NO_3-initiated chemistry. One possibility is that this factor represents two distinct sources or processes that were not fully separated by PMF. Alternatively, the bimodal structure may reflect the intrinsic behavior of a single group of compounds influenced by multiple oxidation regimes.

To investigate this, we first examined the evolution of D2-AVOC-II across PMF solutions with increasing numbers of factors (from 8 to 20). As shown in Fig. R3, the mass spectral and temporal characteristics of this factor remain largely consistent throughout the solutions, and no clear separation into two distinct factors occurs, even at high factor numbers. Further increasing the number of factors risks splitting other well-defined factors.

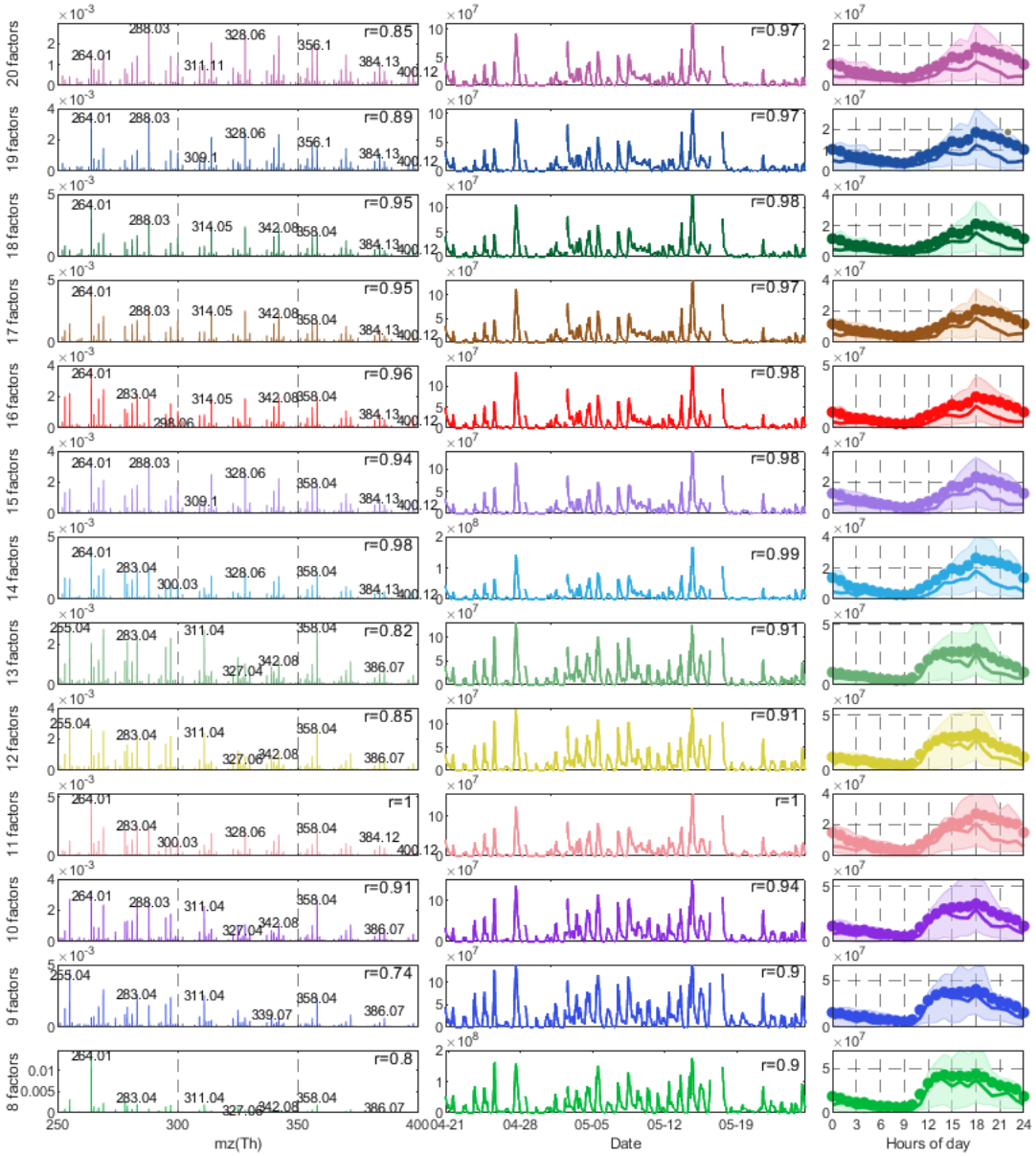

Figure R3. Evolution of the D2-AVOC-II factor (in Range 2) across binPMF solutions with 8 to 20 factors. For each solution, the corresponding mass spectrum (left), time series (middle), and diurnal profile (right) are shown. Correlation coefficients (r) represent the similarity of both the mass spectra and time series compared to the corresponding factor in the selected 11-factor solution.

Additionally, we analyzed the diurnal patterns of CHO and CHON species within D2-AVOC-II. As shown in Fig. R4, both classes exhibit bimodal behavior, with significant contributions during both daytime and nighttime. This indicates that the bimodality is not caused by the accidental merging of two unrelated factors, but rather reflects the intrinsic temporal dynamics of the compounds grouped in D2-AVOC-II.

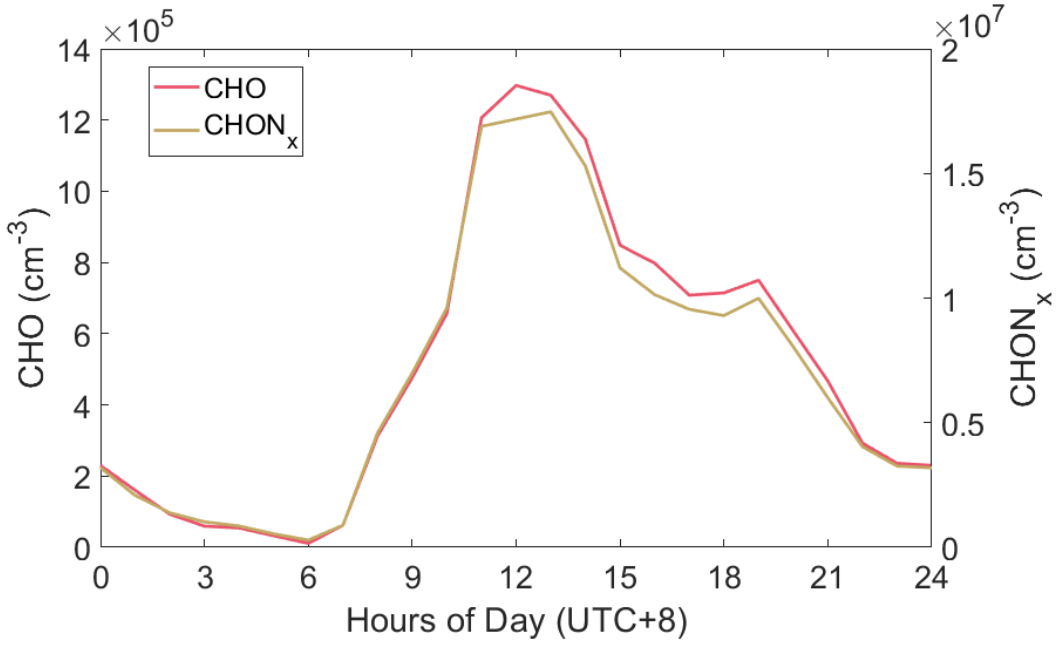

Figure R4. Median diurnal variations of CHO and $CHON_x$ species of D2-AVOC-II

Taken together, these results suggest that D2-AVOC-II is a coherent factor characterized by contributions from both photochemical and nighttime NO_3 oxidation pathways, rather than an unresolved combination of two separate sources.

Lines 326-327. The statement "higher nighttime values are observed, suggesting some transport influence" is unclear to me. Why does nighttime indicate transport? You've identified a transport factor, so did you find some common compounds? Nighttime concentrations could also result from some sources or compounds with relatively high volatility that linger after daytime formation.

Response:

Thank you for the valuable comment. We agree that our initial suggestion of transport influence based on higher nighttime values may not be fully justified. Upon further reflection, we acknowledge that there is no direct link between nighttime peaks and transport. Although we did identify a transport factor (Trans_AVOC), and some compounds such as $C_xH_{2x-1,2x-3}O_6N$ and $C_xH_{2x-2}O_8N_2$ are present in both the transport factor and the D4-AVOC-IV factor, these compounds are also observed in other AVOC-related factors, indicating that they are not exclusive to transport.

Upon further analysis, we found that the nighttime enhancements of this factor during certain periods (e.g., P0 in Fig. R5) coincide with elevated O_x (O_3 + NO_2) levels. Since O_x is less affected by nocturnal NO titration than O_3 alone, it serves as a more robust indicator of photochemically aged air and regional background influence. This co-variation suggests that some of the nighttime enhancements may be associated with

transport influence. But given the factor's distinct diurnal pattern with clear daytime peaks and lack of clear transport signatures, we consider transport influence to be minor and have removed this speculation in the revised text to avoid potential misinterpretation.

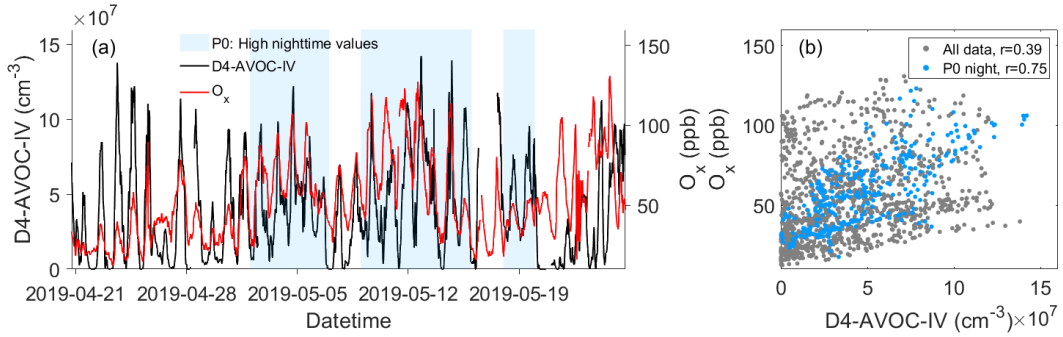

Figure R5. (a) Time series of the D4-AVOC-IV factor (black) and O_x (red) with blue shaded areas representing periods of high nighttime values (P0) identified for further analysis. (b) Correlation between D4-AVOC-IV and O_x, with blue points representing nighttime data (18:00-6:00 LT) during the P0 period.

Line 345. Could these C10 compounds be partly formed through C5-RO2 + C5-RO2 rather than from monoterpene, because they are grouped in this Isoprene-related factor by PMF? Similarly, for section 3.3.4, factor N4-SQT, could there be C15 compounds formed from C5-RO2 + C10-RO2 dimer?

Response:

We greatly appreciate this insightful suggestion. The potential formation of C_{10} and C_{15} compounds through dimerization of different RO_2 radicals (e.g., C_5-RO_2 + C_5-RO_2 or C_5-RO_2 + C_{10}-RO_2) is indeed a plausible pathway, particularly under nighttime conditions at our site, where we observed substantial concentrations of both $C_5H_8NO_5$ and $C_{10}H_{16}NO_x$ RO_2 radicals. However, for the D5-IP factor, which is primarily a daytime factor, RO_2 radicals are expected to terminate predominantly via reaction with NO rather than through bimolecular RO_2–RO_2 reactions. This makes significant dimerization within this factor less likely, although we cannot completely exclude the possibility.

In contrast, the N4-SQT factor is a nighttime factor, and thus RO_2–RO_2 reactions could plausibly contribute to the formation of certain C15 species. Nevertheless, we also observe $C_{15}H_{24}NO_x$ compounds that can be attributed to the oxidation of sesquiterpene precursors. Therefore, while we cannot rule out the contribution from dimerization (e.g., C5-RO_2 + C10-RO_2), the presence of sesquiterpene-derived RO_2 supports the interpretation that these C15 products are at least partly derived from SQT oxidation.

We have revised the manuscript accordingly to incorporate this discussion and to reflect the mechanistic uncertainty.

Revised text:

Page 13, Line 438-440: Due to the relatively high NO concentration during the daytime at this site, it is unlikely that these C_{10} substances originate from C_5 RO_2+C_5 RO_2.

Page 15, Line 511-517: However, some of the $C_{15}H_{24}O_xN_2$ species, particularly those with higher oxygen content, are likely products of C_5-RO_2 and C_{10}-RO_2 dimerization reactions, given the presence of $C_5H_8NO_5$ and $C_{10}H_{16}O_xN$ radicals observed in other nighttime factors and their similar diurnal patterns. However, due to the detection of C_{15} RO_2, these C_{15} substances are more likely to originate from sesquiterpene precursors.

Lines 360-361. A repeated sentence, "This RO2 360 radical originates from NO3-initiated oxidation of isoprene."

Response:

We thank the reviewer for pointing this out. The redundant sentence has been removed in the revised manuscript.

Figure 2. It would be helpful for readers if you could label each factor with the molecular formulae of their highest peaks for quick visual reference (e.g., a quick glance at the C numbers). Also, a pie chart showing the contribution of each factor to the total signal intensity could be informative.

Response:

We thank the reviewer for the helpful suggestion. As recommended, we have revised Figure 2 to include molecular formula labels for the highest peaks of each factor, allowing for a quick visual reference to their dominant carbon numbers and chemical compositions. In addition, a pie chart summarizing the contribution of each factor to the total signal intensity has been added to the Supplementary Information (Fig. S6). These additions enhance the clarity of the figure and provide a more intuitive overview of the chemical composition and relative importance of each factor.

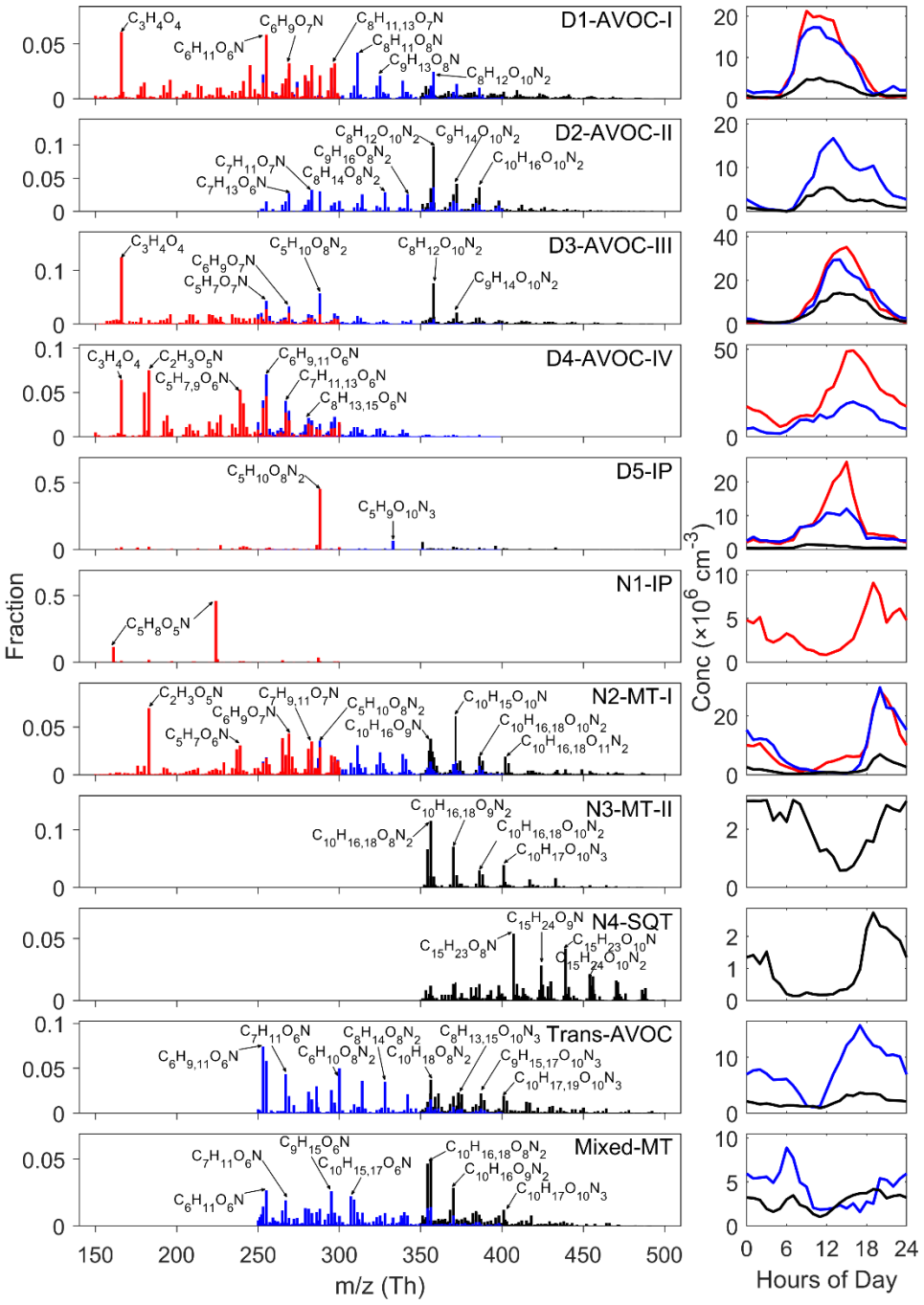

Figure 2. Mass spectral profiles and median diurnal variations of the selected binPMF factors, and the elemental formulas of major peaks are labeled above them. Factors describing the similar process were assembled, red for Range 1, blue for Range 2 and black for Range 3.

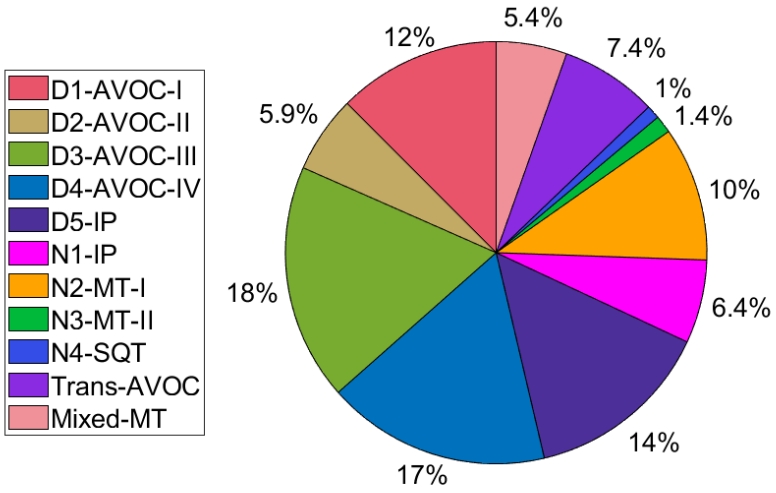

Figure S6. Relative contributions of the 11 factors to the total concentration of measured OOMs.

Lines 396-397. Can you provide plots for the diurnal variation of dinitrates $C_{10}H_{16,18}O_{8-13}N_2$ and trinitrates $C_{10}H_{17}O_{10-13}N_3$? The diurnal plot of this factor will be the average of all organic nitrate, while the dinitrates (NO_3-RO_2 + NO or monoterpenes contain two C=C bonds that reacted twice with NO_3?) and trinitrates (further oxidation of dinitrates?) should only appear in the early morning, based on your hypothesis, right?

Response:

Thank you for the constructive comment. We have now added the diurnal variation plots of dinitrates ($C_{10}H_{16,18}O_{8-13}N_2$) and trinitrates ($C_{10}H_{17}O_{10-13}N_3$) as Fig. R6. Contrary to the hypothesis that these species should appear only in the early morning, our results show that both dinitrates and trinitrates exhibit broader temporal distributions.

It is also important to note that these C10 compounds are not exclusive to the N3-MT-II factor; other factors contribute to them to varying degrees. Therefore, their diurnal variations reflect a combination of sources and cannot be taken as representative of the N3-MT-II factor alone. In contrast, the PMF analysis groups species based on their co-variation across time, and the N3-MT-II factor as a whole shows a consistent nighttime-to-early-morning profile. We hypothesize that these compounds could be secondary oxidation products from nocturnal processes, such as the initial oxidation by NO_3 radicals, followed by further OH radical-driven oxidation in the morning. Similarly, some of the nighttime concentrations might be the result of daytime oxidation products that undergo additional NO_3-initiated oxidation during the night. Overall, the N3-MT-II factor represents a multi-generational oxidation product, involving multiple

oxidants during the transition between day and night. For clarity, I have revised the relevant paragraph in the original text.

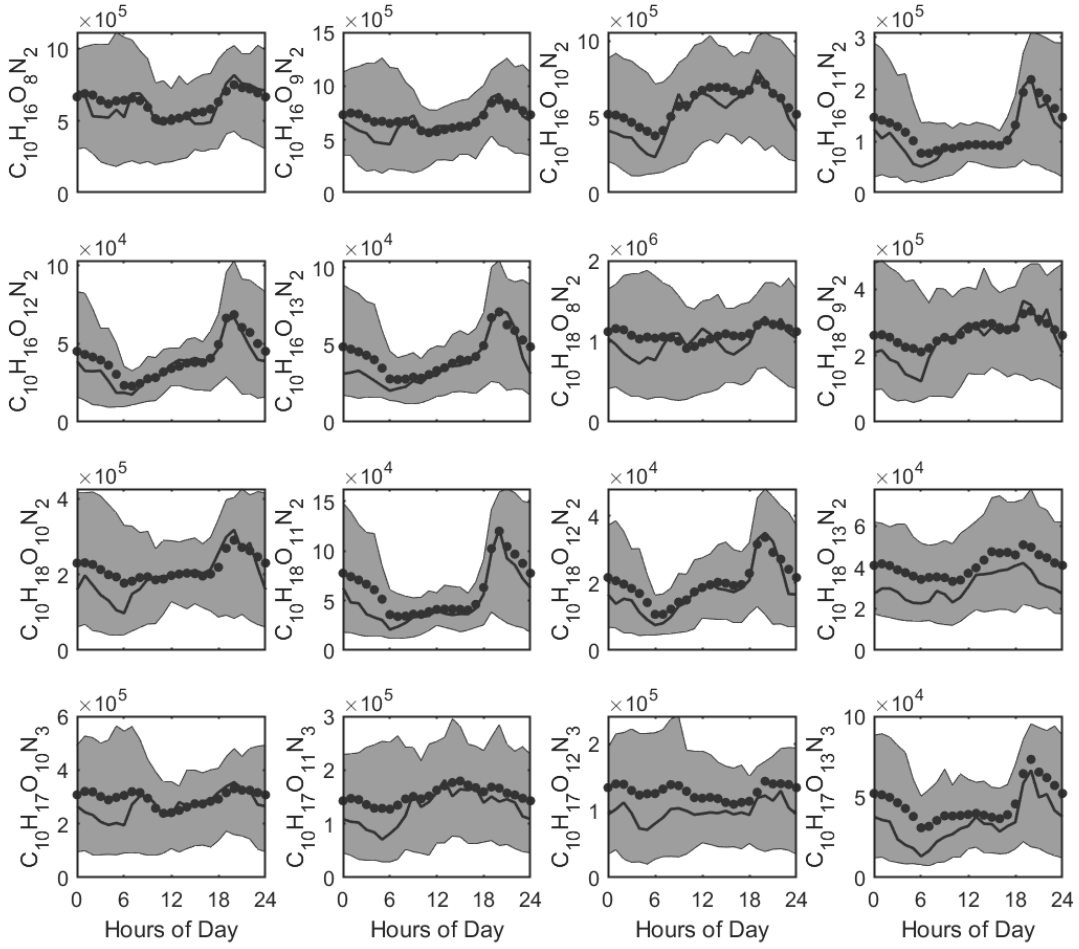

Figure R6. Diurnal variations of C10 dinitrates and trinitrates. Each subplot represents the hourly variation of a specific compound, with the shaded region indicating the interquartile range (between upper and lower quartiles), the solid line representing the median, and the scattered points indicating the mean values.

Revised text:

Page 14, Line 493-503: This suggests that NO_3-initiated oxidation of monoterpenes at night is followed by further oxidation in the morning, potentially involving OH and O_3, leading to the observed multi-nitrate species. Furthermore, some of the nighttime concentrations may arise from daytime oxidation products that undergo additional NO_3-driven oxidation during the night. Overall, this factor represents multi-generational oxidation products, involving various oxidants during the transition between day and night.

Lines 464-467. I don't understand why the sub-range PMF "reveals how chemical conditions and processing pathways evolve over time, reflected by temporal variations in the relative contributions of spectral sub-ranges to individual factors". Like

traditional PMF, your sub-range PMF should also generate static mass spectra for each factor, right? Then, how were you able to obtain mass spectra for factors D3-AVOC-III and D1-AVOC-I under different conditions? Please explain this in your method part as well.

Response:

You are correct that traditional PMF generates static mass spectra for each factor. In our approach, we used a subrange PMF that allows for the identification of factors across different spectral subranges. Each factor is derived from a combination of sub-ranges that exhibit similar temporal variation, grouped together as the same factor. However, due to differences in volatility and chemical composition across subranges, the temporal evolution of the same factor will not be perfectly consistent across all subranges. This can be seen in the correlation coefficients in Fig. 3, where some factors show lower than perfect correlations ($r<1$) across subranges.

As a result, the relative contribution of each subrange to a factor will evolve over time. For factors with contributions from multiple subranges, the mass spectra will vary with time, reflecting these dynamic shifts in the subrange contributions. The more sub-ranges we include, the finer the temporal variation we can analyze, and this may reveal more detailed information about the underlying chemical processes. For example, we provide an analysis of D3-AVOC-III in Fig. R7, showing its average mass spectra for different time periods. The proportion of R1 in (a) is lower than in (b), while the proportion of R3 in (a) is higher than in (b). Our subsequent analysis builds on this dynamic temporal variation to explore the underlying chemical conditions and processing pathways.

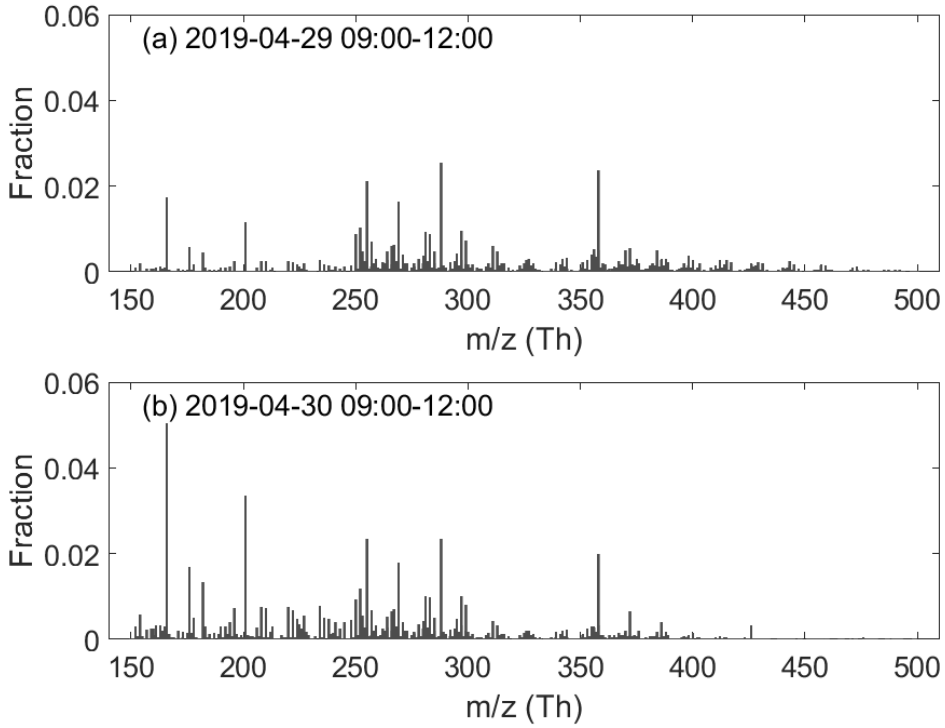

Figure R7. Average mass spectra of the D3-AVOC-III factor during different time periods: (a) 09:00–12:00 on April 29, 2019, and (b) 09:00–12:00 on April 30, 2019.

We will expand on this explanation in the methods section of the revised manuscript to provide more clarity.

Revised text:

Page 6, Line 195-202: The relative changes in the source factor profiles between the different sub-ranges contribute to the dynamic nature of the combined factor spectra. Specifically, variations in the mass spectral features across the sub-ranges lead to distinct temporal and compositional changes in the final factor profiles. This dynamic analysis approach enables better resolution of source processes and provides a more robust representation of the underlying sources. By minimizing sink-induced variations and leveraging the temporal and compositional overlap between the ranges, we achieve improved factor separation and identification.

Page 18, Line 610-617: Specifically, as different sub-ranges are combined, the relative intensities of these ranges fluctuate, demonstrating how variations in chemical reactivity and environmental conditions influence the composition and formation of OOMs. These dynamic observations better represent atmospheric processes, where constantly changing oxidation conditions alter OOM distributions across different volatility ranges. The ability to track these variations in real time allows for a more nuanced understanding of how source and sink processes interact under different atmospheric conditions.

Figures 6 and S6 (and also Figures 7 and S7), what is the unit for "difference of profiles"? Using relative difference (e.g., normalized to "Low T/NOx" or "Low CS") might make the comparison clearer and easier to understand.

Response:

Thank you for your valuable suggestion. We agree that using relative changes would make the comparison clearer and easier to understand. We attempted to replot the figure using the relative difference, and the results indeed lead to the same conclusions. However, the new plot (Fig. R8) is not as visually appealing, as most of the peaks are clustered around similar values. Upon analyzing this result, we found an explanation. The relative difference after normalization is a ratio form (H-L)/L=H/L-1, and for single-range PMF factors, the spectra for any two time periods are identical. Therefore, the ratio of the peak values between any two time periods is constant. As a result, parts of the plot corresponding to mass ranges with only one PMF analysis (150-250 Th, 300-350 Th, and 400-500 Th) show a constant value. Some peaks deviate from this constant value because concentrations below the detection limit were excluded for certain peaks. Ultimately, we decided to retain the original plotting method.

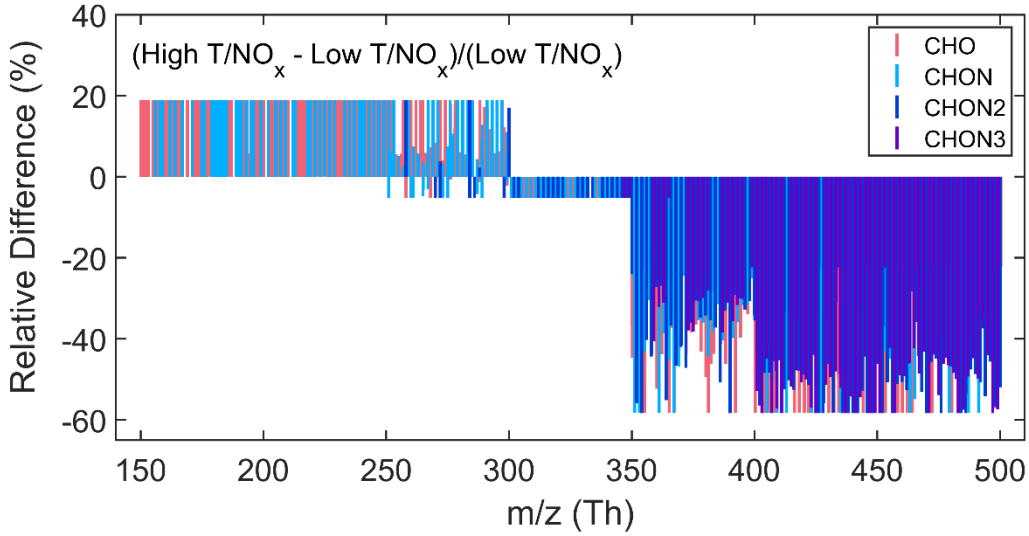

Figure R8. Relative difference between the average mass spectra of D3-AVOC-III under high T/NO_x (above the upper quartile) and low T/NO_x (below the lower quartile) conditions, normalized to low T/NO_x.

Line 497. What exactly is the "T/NOx ratio"? They have different units, so, the meaning of this ratio is unclear. What does a high or low value indicate chemically or physically? Why not directly use T or NOx, or make one plot vs T but colored by NOx, for example?

Response:

Originally, our intention was to separately investigate the effect of temperature on nitrogen-containing OOMs. As shown in Fig. R9, the trends observed using temperature alone are largely consistent with our main conclusions. However, analyzing temperature in isolation is not entirely comprehensive, since NO_x levels also play a crucial role in determining the nitrogen content of oxidation products. To better isolate the temperature effect under comparable NO_x levels, we adopted a ratio-based approach (T/NO_x). While not dimensionally rigorous, this metric conceptually represents the influence of temperature under a fixed NO_x condition—essentially, "how temperature modulates nitrogen incorporation into OOMs when NO_x availability is constrained." This simplification allowed us to group the data more clearly by combined chemical conditions, facilitating interpretation. That said, we agree this representation may be confusing, and we have added clarification in the revised text.

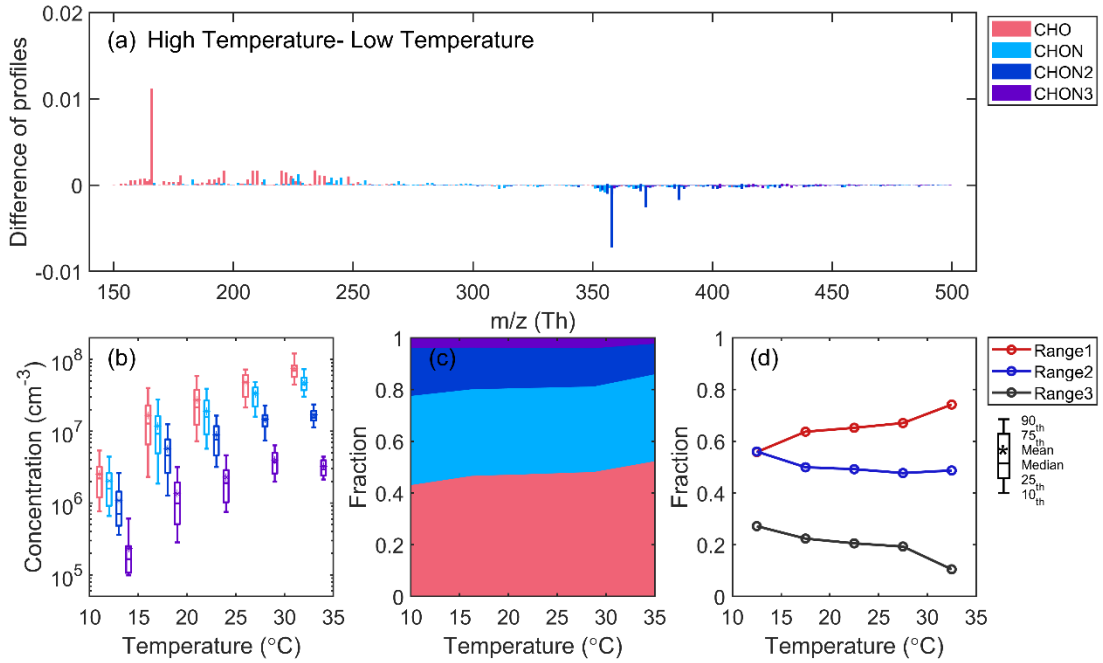

Figure R9. Characteristics of D3-AVOC-III under varying temperature conditions. (a) Difference between the average mass spectra of D3-AVOC-III under high temperature (above the upper quartile) and low temperature (below the lower quartile) conditions. (b) Boxplots of the concentrations of CHO and $CHON_x$ (x = [1,3]) species binned by temperature in each 5 °C interval. (c) Fractional contributions of CHO and $CHON_x$ (x = [1,3]) species for different temperature conditions. (d) Evolution of fractional contributions of three sub-ranges as a function of temperature.

Revised text:

Page 19, Line 642-652: While temperature and NO_x individually influence oxidation chemistry, analyzing them in isolation may obscure their combined effects—especially since NO_x levels tend to decrease with increasing temperature due to enhanced photochemical activity and atmospheric mixing. To better isolate the influence of temperature under comparable NO_x conditions, we adopted the ratio of temperature to NO_x (T/NO_x) as a simplified metric. Although this ratio does not represent a physically defined parameter, it serves as a practical index allowing for clearer grouping of data and a more interpretable assessment of compositional differences.

Lines 510-512. Do you have references to support this argument that "elevated temperatures favor the RO + NO_2 channel, reducing the formation of $RONO_2$ from the RO_2 + NO reaction"? Should the product of RO+NO_2 also be thermally unstable? Why does higher T favor RO + NO_2 than RO_2 + NO?

Response:

Thank you for pointing this out. We are sorry for the confusion caused by our wording — the term "RO + NO_2 channel" was a misstatement. Here, our discussion refers specifically to the reaction between RO_2 and NO, which primarily proceeds via two branches:

$$RO_2 + NO \rightarrow RO + NO_2 \qquad R1a$$

$$RO_2 + NO \rightarrow RONO_2 \qquad R1b$$

Experimental studies have shown that the branching ratio of the $RONO_2$ formation pathway (R1b) decreases with increasing temperature, meaning that elevated temperatures favor the RO + NO_2 pathway (R1a) over the $RONO_2$ formation (R1b). This temperature dependence has been quantified in several studies (Cassanelli et al., 2007; Butkovskaya et al., 2010; Perring et al., 2013). The observed decline in nitrogen-containing compound fractions under higher temperature conditions in our data is consistent with this known chemical behavior. We will revise the original sentence for clarity and include the appropriate references in the manuscript.

Revised text:

Page 20, Line 663-668: This trend reflects shifts in RO_2 radical chemistry. Under high NO_x conditions, RO_2 primarily reacts with NO, and this reaction has two main pathways: formation of RO + NO_2 or organic nitrates ($RONO_2$). Previous studies have shown that increasing temperature suppresses the nitrate-forming branch in favor of the RO + NO_2 branch, thus reducing the formation of $RONO_2$ (Cassanelli et al., 2007; Butkovskaya et al., 2010; Perring et al., 2013).

Line 554. What is the typical range of CS observed at your site? Is 0.05 s^{-1} considered extremely high in your context?

Response:

The CS values observed during the campaign ranged from 0 to 0.05 s^{-1}, with 0.05 s^{-1} being at the upper end of the distribution. To clarify this point, we have added the corresponding time series and diurnal pattern of CS (Fig. R10).

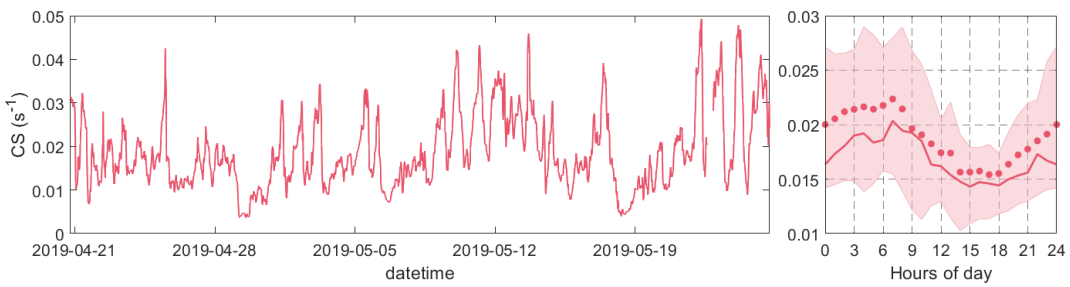

Figure R10. Time series and diurnal variation of the condensation sink (CS) during the campaign.

Lines 558-559. The sentence "condensation processes under high CS conditions act as a controlling mechanism for species partitioning" is very confusing? Should volatility and OA mass always control the gas-particle partitioning? And CS means condensation sink, of course under higher CS one would expect higher rate of condensation? Please clarify.

Response:

Thank you for pointing out the ambiguity. The original sentence was indeed unclear and may have been misleading. Our intention was not to refer to gas-particle partitioning, which is governed primarily by volatility and OA mass, but rather to describe the relative abundance of gas-phase OOMs with different volatilities as a function of the condensation sink (CS).

Specifically, at low CS levels, the increase in OOM signals is primarily driven by enhanced chemical formation, and species across a wide volatility range show simultaneous increases. However, at high CS levels, condensation loss starts to dominate over chemical production, particularly for low-volatility OOMs. As a result, the relative contribution of lower-volatility compounds begins to decline, whereas semi-volatile compounds remain more abundant in the gas phase.

We will revise the original sentence accordingly to improve clarity and remove the confusion around partitioning processes.

Revised text:

Page 22, Line 729-732: This observation aligns with prior theoretical predictions and laboratory findings (Peräkylä et al., 2020), which suggest that under high CS conditions, condensation dominates over chemical formation in shaping the gas-phase abundance of different volatility classes of OOMs.

Figures 6d and 7d. What does this fractional contribution analysis mean? Because at each CS bin, the sum of R1, R2, and R3 seems to be larger than 1, which is confusing. Also, your explanation in lines 561-564 is misleading. With the increases in CS, all mass ranges should decrease because of enhanced condensation, right? It is because R3 and R2 condensed more than R1, making the relative fraction of R1 increase. Therefore, I think absolute concentrations would be more informative than fraction contributions here.

Response:

We appreciate the reviewer's constructive comments and the opportunity to clarify. The "fractional contribution" in Figs. 6d and 7d refers to the relative contribution of each spectral sub-range to the total signal within the entire analyzed mass range (150–500 Th). Due to the intentional 50 Th overlaps between adjacent sub-ranges (e.g., 250–300 Th and 350–400 Th), the summed concentrations of all sub-ranges exceed the total,

resulting in fractional contributions summing to values greater than 1. We have now added a clarification on this point.

In response to the reviewer's suggestion, we also generated alternative plots showing the absolute concentrations of R1–R3 as functions of temperature/NO_x and condensation sink (Fig. S12). These results confirm our previous interpretation: all sub-ranges of D1-AVOC-I increase with CS initially, consistent with pollution-driven chemical production. However, under very high CS conditions, R2 and R3 begin to decline, while R1 continues to increase, indicating a volatility-dependent loss from the gas phase due to condensation. Thus, both the fractional contribution and absolute concentration perspectives are complementary and valuable. We agree that the original explanation may have been misleading and have revised the relevant text to more accurately reflect the interplay between production and condensation.

Revised text:

Page 22, Line 733-741: We analyzed the fractional contributions of different sub-ranges under varying CS conditions. Due to their lower volatility, higher m/z species in R2 and R3 are more susceptible to loss through condensation under high CS, while lower m/z species in R1 (likely SVOCs and LVOCs) are less affected. As a result, the relative contribution of R1 increases with CS, whereas those of R2 and R3 gradually decrease. This trend highlights a volatility-dependent partitioning effect, where enhanced condensation preferentially removes less-volatile compounds from the gas phase under elevated CS conditions, as also reflected by the absolute concentration changes of sub-ranges under increasing CS (Fig. S12).

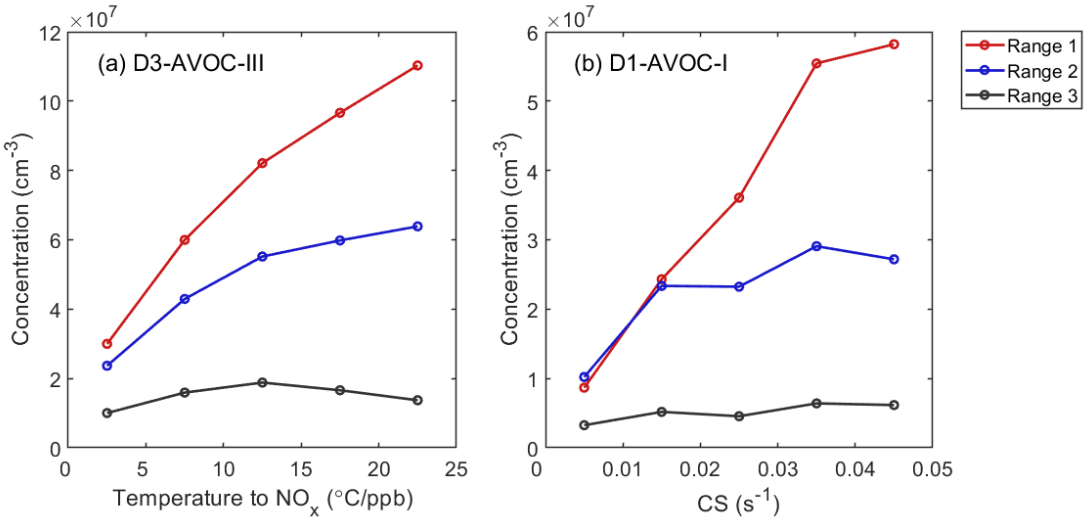

Figure S12. Evolution of concentrations of three sub-ranges of (a) D3-AVOC-III with T/NO_x ratio, and (b) D1-AVOC-I with CS.

Reference:

Butkovskaya, N., Kukui, A., and Le Bras, G.: Pressure and Temperature Dependence of Ethyl Nitrate Formation in the $C_2H_5O_2$ + NO Reaction, J. Phys. Chem. A, 114, 956–964, https://doi.org/10.1021/jp910003a, 2010.

Cassanelli, P., Fox, D. J., and Cox, R. A.: Temperature dependence of pentyl nitrate formation from the reaction of pentyl peroxy radicals with NO, Phys. Chem. Chem. Phys., 9, 4332, https://doi.org/10.1039/b700285h, 2007.

Hyttinen, N., Kupiainen-Määttä, O., Rissanen, M. P., Muuronen, M., Ehn, M., and Kurtén, T.: Modeling the Charging of Highly Oxidized Cyclohexene Ozonolysis Products Using Nitrate-Based Chemical Ionization, J. Phys. Chem. A, 119, 6339–6345, https://doi.org/10.1021/acs.jpca.5b01818, 2015.

Kürten, A., Rondo, L., Ehrhart, S., and Curtius, J.: Calibration of a Chemical Ionization Mass Spectrometer for the Measurement of Gaseous Sulfuric Acid, J. Phys. Chem. A, 116, 6375–6386, https://doi.org/10.1021/jp212123n, 2012.

Peräkylä, O., Riva, M., Heikkinen, L., Quéléver, L., Roldin, P., and Ehn, M.: Experimental investigation into the volatilities of highly oxygenated organic molecules (HOMs), Atmos. Chem. Phys., 20, 649–669, https://doi.org/10.5194/acp-20-649-2020, 2020.

Perring, A. E., Pusede, S. E., and Cohen, R. C.: An Observational Perspective on the Atmospheric Impacts of Alkyl and Multifunctional Nitrates on Ozone and Secondary Organic Aerosol, Chem. Rev., 113, 5848–5870, https://doi.org/10.1021/cr300520x, 2013.

Riva, M., Rantala, P., Krechmer, J. E., Peräkylä, O., Zhang, Y., Heikkinen, L., Garmash, O., Yan, C., Kulmala, M., Worsnop, D., and Ehn, M.: Evaluating the performance of five different chemical ionization techniques for detecting gaseous oxygenated organic species, Atmos. Meas. Tech., 12, 2403–2421, https://doi.org/10.5194/amt-12-2403-2019, 2019.